technical memorandum Daresbury Laboratory

DL/SCI/TM47A

SRS CAVITY MICROWAVE WINDOW FAILURE INVESTIGATION:
PRELIMINARY PROBLEM ANALYSIS AND LITERATURE REVIEW

by

R.A. RIMMER

MARCH, 1986

RIMM-86/25

Science & Engineering Research Council

Daresbury Laboratory

Daresbury, Warrington WA4 4AD

Abstract

This report gives a broad analysis of the nature of the cavity microwave window failure problems experienced by Daresbury SRS and some microwave tube manufacturers and examines the possible mechanisms involved with a review of the relevant literature. It also suggests the directions in which research should proceed to understand and model the failures better, with the ultimate aim of systematic eradication of the problem.

CONTENTS

1. DESCRIPTION OF SYSTEM

1.1 Introduction

High power windows are used at radio and microwave frequencies in a wide variety of devices and applications in industry and research. Such windows are prone to failure, apparently due to internal stresses caused by heating or due to electrical breakdown caused by surface charging. The heating cannot always be explained solely by dielectric loss within the window and a variety of mechanisms have been postulated to account for the additional heat input.

The particular applications relevant to this study are the use of microwave windows to couple r.f. power into the Daresbury Synchrotron Radiation Source (SRS) and to couple power out of high power klystrons manufactured by various companies in the UK and elsewhere, although techniques used and analysis produced should be applicable to a much wider range of situations.

The Daresbury SRS employs large alumina or beryllia discs to couple substantial amounts of r.f. power (theoretically up to 100 kW per window) from waveguide at atmospheric pressure into each of the four evacuated accelerator cavities. Thus the window forms part of the vacuum envelope and is subjected to atmospheric pressure in addition to any thermal stress.

Microwave tube makers use cylindrical alumina windows to couple power in and out of klystron resonant cavities. The cavities are bounded insided the window by the cavity plates and nose cones of the drift tubes and outside the window by tuneable cavity boxes to allow use of the klystron over the maximum frequency band. In the case of klystrons it is usually only the output window which suffers excessive heating or charging effects because, being primarily an amplifier device with a high gain, the fields in the output cavity are much greater than in the other cavities.

In both cases window failure ultimately limits the maximum power handling capability of the system, although it is often only one of a number of effects that limit high power operation.

This report attempts to outline the problems affecting window performance, taking the SRS as the initial target for investigation, and to indicate areas where investigation should be undertaken to try to understand the mechanisms involved and ultimately to improve performance. Parallels and contradictions betweene the SRS and klystron window problems will be noted wherever possible.

1.2 Window Assemblies

The SRS windows are mounted as in fig.1 in a copper ring fixed in a water-cooled flange. This is mounted in a short circular tube linking the toroidal cavity to the narrow wall of the guide. In some analyses this is considered to be a short length of circular waveguide which is below cut-off at the SRS operating frequency (~ 500 MHz) although in reality it is neither a waveguide nor a thin iris but somewhere in between. Being a large hole, taking up most of the short side of the waveguide, conventional small aperture theory cannot be directly applied and more complex techniques must be used (see section 3.4). Window failures have been reduced by moving the window assembly to a higher position in the tube where it is in a less intense field and some analysis to support this move has been performed[1], but this is at the expense of the maximum available coupling factor which has halved although it is still sufficient for current requirements.

Coupling, which is magnetic, is varied by moving a sliding short circuit in the waveguide which effectively moves the standing wave pattern up or down the guide. Maximum coupling occurs when there is maximum magnetic field over the window (this does not correspond to the "magnetic field maximum" in the conventional sense, i.e. at the centre of the waveguide, which is one quarter of a wavelength away, see fig.2). At this point the electric field is also at a maximum, but 90° ($\pi/2$ rad) out of phase with the magnetic field which may provide conditions for multipactor or ion trapping.

A typical klystron window is mounted as in fig.3 with the cavity crossing the vacuum envelope at the window. The tube body often has water cooling (primarily to dissipate heat caused by body current) which helps to cool the cavity end plates, while the external cavity is usually forced-air cooled. Coupling out of the cavity is achieved by a variable loop antenna. The kly-

stron cavities have an additional static magnetic field along the beam axis, for focusing which affects the conditions for multipactor etc., but since the window is comparatively close to the centre of the cavity it does not intercept much of the r.f. magnetic field. Some work, notably by Priest and Talcott[2] neglects this r.f. field altogether, others[3] have shown that further out in the cavity the magnetic field bends the electron trajectories slightly, modifying the multipactor conditions.

Both applications have tried using beryilia ceramics at some stage or other when heating or mechanical problems have arisen but in view of the potential hazard (especially if broken or abrased, releasing dust) other solutions have always been sought whlch allow the continued use of alumins.

1.3 Properties of Window Materials

Alumina and beryllia are the most commonly used dielectric materials for large microwave windows. Both are fabricated into discs or cylinders by a sintering process.

1.3.1 Mechanical and thermal properties of alumina and beryllia

Table 1 shows the common mechanical and thermal properties of alumina and beryllia and their variation with temperature. From these figures it can be seen that alumina is a tougher material with higher tensile strength, compressive strength and modulus of elasticity but that beryllia is a much better conductor of heat, hence its use in environments where alumina cannot disperse heat fast enough (allied to its lower dielectric loss which generates less heat too - see section 1.3.2)

It is important that with both materials not only does the mechanical strength degrade at higher temperatures but the thermal conductivity drops. This, coupled with an increase in dielectric losses can lead to a thermal runaway situation, rapidly leading to window failure through excessive thermal stress.

1.3.2 Electrical properties of alumina and beryllia

Dielectric constant of both materials is temperature and frequency dependent. Figures from different sources[4,5] show a slight drop in dielectrlc constant at higher frequencies, but an increase with increasing temperature (see Table 2).

Dielectric loss appears to increase with temperature and frequency for alumina. Although figures are not readily available for beryllia it is not unreasonable to suppose that it might behave similarly.

Dielectric breakdown. Beryllia is marginally better than alumina at holdlng off a D.C. voltage (see table 2) but the breakdown field strength seems to be very dependent on the size and construction of the sample (small samples seem to withstand higher field strengths) perhaps due to imperfections in the larger samples.

Alumina has a higher dielectric constant and loas tangant then beryllia at all temperatures and frequencies for which data are available. Both have extremely high ohmic resistance at normal operating temperatures but beryllia has the better D.C. breakdown voltage. On these criteria beryllia is better suited to the application of high power windows on electrical as well as thermal grounds but it is rarely used where alumina is a viable alternative for reasons of safety (BeO dust), cost and mechanical ntrength.

1.3.3 Secondary electron emission

Uncoated windows of beryllia or alumina have secondary emission coefficlents (SEC) greater than unity for a wide range of primary electron energies and angles of incidence (see Table 3) which can give rise to secondary electron resonancs phenomena, e.g. multipactor, under a wide range of conditions (see loss mechanisms, section 2.6). Various surface treatments have been tried to reduce or eliminate this condition (see section 2.6).

2. LOSS MECHANISMS

2.1 General

In a complex environment such as the SRS r.f. system or a high power klystron output window assembly, the r.f. loss and subsequent window heating are due to a combination of different mechanisms of varying importance.

These in turn are often susoeptible to conditions of operation, geometry of the syetem, surface conditions etc. resulting in a complicated overall picture. This seotion gives a brief outline of the possible loss mechanisms and their importance.

2.2 Dielectric Loss

The simplest mechanism of converting r.f. power to heat is straightforward loss due to the bulk properties of the non-ideal dielectric. In both applications the field strengths are high so even a small loss tangent (see Table 2) can cause quite severe heating. Being in general rather poor conductors of heat and having mechanical and electrical properties with notable temperature dependences, this is a potentially unstable situation. Thermal runaway is possible leading to window failure through internal stress caused by internal temperature gradients.

E.A. Hughes[6] and D.M. Dykes and T. Garvey[1] have investigated the dielectric loss heating in the SRS windows. Hughes assumed the window aperture to be a short length of circular waveguide cut off at 500 MHz but transmitting in the TE_{11} mode with very high attenuation, and attempted to estimate the distribution of heating over the surface to try to explain observed surface markings (the so-called tiger skin mark). Dykes and Garvey applied a low power perturbation technique, drawing a dielectric bead across the window surface, to look at the field distributions and estimate the peak electric field strengths. Their results[7] show substantial heating in the two possible window positions, nearly 600 W absorbed (from 40 kW input) in the lower position (i.e. nearest the high cavity fields) but still nearly 250 W in the upper position (i.e. nearest the waveguide). Although these are quite high the heat dispersion properties of the system are such that this alone is rarely sufficient to break a window but ie a major contributor to overall heat input.

2.3 Ohmic Loss

Under normal conditions the ohmic resistance of the bulk ceramic is extremely high so there is negligible power absorption due to "I^2R" heating. However, it has been observed that windows taken out of the SRS have developed regions near the centre of the window of increased conductivity. Dykes and Garvey and others have observed surface resistances as low as 10 MΩ per square corresponding to the area known as the "tiger skin" marking. Dykes and Garvey calculated that several tens of watts could be dissipated in this region (up to ~ 70 W max.) over a very small area. This may be sufficient to cause critical stress levels when combined with dielectric loss under conditions of very high power throughput, but under normal conditions it would appear that a further mechanism is still required to produce a thermal runaway situation. The white spot sometimes observed just before failure could conceivably be due to excessive local heating changing the nature of the surface, maybe even melting it.

There are several theories (as yet largely unproved) of the formation of these films. It is possible that they may arise because of some form of ion trapping or be due to a chemical reaction between some of the trace elements found in the vacuum vessel, e.g. volatile organic copper compounds, as suggested by Keller and Körösy[8].

So far, various analytical techniques have been used to try to identify the chemical nature of the surface films but have been inconclusive. Because of the size of the windows only fragments can be fitted into apparatus such as scanning electron microscopes (SEM) which is an additional hindrance to the analysis.

It is planned to continue some experimental work to compare the losses of coated windows with uncoated ones by looking at the change in Q of a resonant structure in which the window sits at an electric field maximum. This technique is not yet reliable, however, and will not be described further at this stage.

2.4 Multipactor

A lot of work has been done investigating the properties of multipactor discharges. This section is intended to be a brief résumé of the relevant ideas and results.

Hatch and Williams[9] and Gill and von Engel[10] amongst others develop-

ed the theory of multipactoring between two metal electrodes or a pair of surfaces with an externally applied electric field, under conditions of very low gas pressure, i.e. approaching a good vacuum. Multipactoring is a secondary electron resonance phenomena where an electron is emitted at a suitable phase in the r.f. cycle, is accelerated across the gap, and impinges on the second electrode with a transit time of an odd number of half-cycles (to preserve the phase condition) and sufficient energy to release more than one secondary on average (to maintain or increase the discharge). It has been shown analytically and experimentally that multipactor may occur for a wide but finite range of voltage and phase conditions for a given geometry, and is dependent on the secondary emission properties (and hence surface condition) of the electrodes. Electron bombardment by multipactoring can absorb large amounts of r.f. power and convert it into heat at the surface(s) involved to a degree where outgassing can occur, giving rise to visible glow discharges and even direct gas breakdown. Multipactor has been observed in a wide range of equipment and devices[11] and has formed the basis for some new devices[12].

Several experimentors have postulated and observed multipactor on a single surface, with a d.c. bias across the gap to maintain a suitable phase condition[13], or in the presence of a magnetic field which returns the electrons to their starting surface[14]. Priest and Talcott[2] describe electron resonance on klystron output windows, with and without a magnetic field, of a type which may have direct relevance to this study. In the case of the klystron window, with a strong axial magnetic field, a sustained single-surface multipactor can exist which can produce a substantial heating effect and may also go a long way to explaining observed window charging phenomena. If a large number of multipacting secondary electrons can be shown to migrate across an insulator surface, residual charge could be quite substantial. Klystron windows are known to suffer puncturing, thought to be due to direct dielectric breakdown due to surface charging.

SRS windows have been observed to suffer a similar charging effect, leading to arcing on the air side of the window. These arcs may occur from the window to the waveguide or even between two points on the window surface. Occasionally these small sparks have triggered breakdown of the waveguide electric field with damaging results. Arc detectors are now fitted in some

parts of the r.f. system of the SRS to trip out the r.f. supply in this case.

In a typical klystron the magnetic field arises because of the need to focus the electron beam down the tube. In the SRS the window is more remote from the beam but is likely to be affected by stray magnetic fields from steering or focussing magnets, cables etc. This makes the system harder to analyse because whereas the klystron has a well-defined axial field, the stray fields around the SRS cavities are much harder to predict. Furthermore, they may vary between cavities and with the set-up of the ring, e.g. the magnet settings may vary depending on the steering geometry or with the use of "wigglers" etc. to vary the synchrotron radiation.

Thus mechanisms are possible in the SRS cavity for two-surface multipacting between the vacuum side of the window and parts of the cavity or window aperture, and single-surface multipacting on the window in the presence of stray magnetic fields or electrostatic bias due to window charging.

Any attempt to analyse or predict the multipactor behaviour of a system such as the SRS window assembly must obviously consider the secondary emission properties of the surfaces involved (see section 2.6) and attempt either analytically or numerically to track electron trajectories around the system. For simple two-surface or single-surface with static bias or magnetic field an analytical solution is possible but with fields changing with time and distance the problem rapidly becomes too complex and computer numerical analysis is the easiest way to obtain a solution (see section 3.5).

More recent investigations tend to concentrate on multipactor effects and their inhibition in accelerator structures[15] and superconducting cavities[16] or the effects of multipactor on components for feeding power into the new generation of plasma containment vessels for fusion reactors[17]. Gallagher recently produced two useful papers[18] condensing much of the known work on multipactor phenomena and has also suggested a multipactor electron gun design[19]. Other authors have produced a variety of multipactor-based devices including switches etc.[20], but these investigations have limited relevance to the SRS/klystron problem. More relevant is the work on secondary electron emission and its inhibition by surface coatings etc. by various authors (see section 2.6).

Various studies have been implemented by companies for NASA[21] on the problems of multipactor in equipment in space, mainly dealing with problems of power loss, noise and distortion in antennae and communications equipment, and for the US Navy[22].

Some further development of multipactor theory was carried out in the USSR in the 1970's, incorporating statistical velocity distribution of the secondary electrons[23].

2.5 X-ray Damage

Although not significantly contributing directly to the heating of the windows, considerable discolouration has been seen of the whole window surface which is presumed to be due to x-rays. X-rays may contribute to multipacting by the production of photoelectrons as they pass through the window. This, or field emission, or electrons lost from the beam and scattered into the cavity could provide the initial primary electron needed to start a multipactor discharge.

Computational techniques have been developed (see section 3.5) which can predict the distribution of x-ray production within a cavity, based on the knowledge of the field distributions within the structure, by tracking an arbitrary number of electrons through many collisions or scatterings and estimating the energy available in such events that might be dissipated in the form of an x-ray photon. From this sort of prediction it is possible to produce an x-ray distribution pattern for the cavity which agrees well with experimental x-ray photographs.

2.6 Secondary Electron Emission

Multipactor can only survive while the field-accelerated electrons have enough energy on impact to release at least one secondary on average, so the obvious method of suppressing multipactor is to ensure that the secondary emission coefficient is always less than unity. Unfortunately this is not the complete story because it has been shown[24] that secondary yield increases with angle (θ) of incidence as sec θ. Thus, grazing incidence of primaries can result in substantially higher secondary emission yields and multipactor

could still occur even if the normal SEC is less than unity. Furthermore there is a demonstrable distribution of secondary energies[25], and hence velocities, which further complicates the multipactor model. Kanaya and Kawakatsu[26] include the contribution of backscattered primary electrons in their analysis of total secondary yield, producing a "universaal" yield-energy distribution curve and an energy distribution for the secondaries. This they tested against experimental measurements with good agreement. Such results may assist realistic modelling of electron trajectories within a cavity over many successive collisions. Dawson[27] gives secondary yield information for some window materials which may be useful. More recently investigation of the secondary emission properties of materials for superconducting microwave cavities has been carried out by Padamsee and Joshi[28] as these materials are of increasing importance in accelerator structures as performance of such machines is increased.

Much work has been done on the development of coatings and surface treatments to decrease the secondary emission yield in waveguides and cavities where multipactor is likely, and some on the inhibition of single-surface multipactor on dielectric windows, notably by Talcott[29] and a series of reports commissioned in the USA[30] the surface modifications over a wide range of treatments including carbon[31,32], titanium[29], copper and gold coatings. These techniques have a two-pronged attack on the problem, firstly using a coating material with a low SEC and also modifying the surface texture to change the discharge properties. Timberlake et al[33] polished the surfaces of waveguides to minimise gas adsorption leading to direct r.f. breakdown and other members of the group[31] later described the use of carbon coatings to lower the SEC to prevent multipactor. They also noted the sec θ dependence of secondary emission with angle of incidence but interestingly that the effect was diminished with a rough surface. Other investigations[17] have gone to great lengths to produce a microscopically rough surface which inhibits secondary emission by increasing the chance of secondaries being recaptured before they escape the surface. This has been proved to be effective in stopping multipactor in evacuated waveguide systems. It is possible that the thin films of copper or gold black applied to the SRS windows inhibit single-surface multipactor in a similar way. The gold coating used by Derfler et al[17] is applied by a complicated chemical and electroplating process, whereas the SRS coatings are applied by evapora-

tion in low pressure inort atmospheres (nitrogen or argon). Talcott reports good success with titanium films although these have been less than successful when tried on SRS windows, primarily through difficulty in obtaining a consistent film with good adhesion. Hayes[30] describes physically modifying the window surface with grooves to reduce the yield.

Secondary and r.f. field emission can be reduced by "conditioning" of surfaces which involves running a cavity or structure initially at low power and increasing the power levels gradually, monitoring the multipactor carefully. At each power level multipacting will generally condition out, eventually enabling high power operation that would not initially be possible. This conditioning will generally persist in the structure provided there is no violent discharge, vacuum incident or contamination to change the nature of the conditioned surface. The SRS cavities need careful conditioning before full power operation can be achieved after the system has been let up to atmosphere, e.g. to replace a window. Halbritter[34] describes an explanation of r.f. conditioning by "electron, photon or He impact which causes hydrocarbon adsorption and dehydrogenation and polymerisation of adsorbed hydrocarbons" which greatly reduces the secondary emission and field emission in superconducting Nb cavities. Understanding the nature of such surfaces may provide clues to multipactor suppression on different materials such as dielectrics and insulators.

2.7 Ion Bombardment

As with any vacuum system there is a finite residual gas pressure in the SRS or klystron, and with a beam running ions will be produced. Indeed, the SRS has clearing electrodes to remove as many ions as possible. Under normal r.f. excitation of a cavity there is no net force on any ion over a suitably long timescale because the high frequency r.f. voltages tend to cancel out due to the relatively large inertia of ions compared to electrons. However, it is possible that static magnetic fields or large static charge on the window could attract or deflect ions towards the window. Under conditions of good vacuum this effect is likely to be small and not contribute noticeably to window heating, but since the individual ions could conceivably have quite high energy they may cause surface damage over a long period of time or may

provide another mechanism for the emission of electrons with sufficient energy to start a multipactor discharge. The vacuum system is not the only source of ions however, during a multipactor discharge it is possible for copper to be sputtered from the cavity wall, and it has even been observed in the SRS that the beam had intercepted something solid in one of the straight sections which had led to sputtering off the stainless steel walls.

3. FIELD MAPPING

3.1 General

In order to attempt any explanation of window heating through dielectric loss, ohmic loss, multipactor etc. it is necessary to know the strength and preferably the direction and distribution of all the electric and magnetic fields involved. In the cases of dielectric and ohmic losses it is then straightforward to calculate the power absorption (see sections 2.2 and 2.3). In the case of multipactor or secondary electron avalance effects a good knowledge of the fields is essential for prediction of electron trajectories and for computer programs to make predictions of measurable discharge effects (see section 3.5).

This section outlines some of the techniques available for analysis or mapping of the fields.

3.2 Perturbation Techniques

Dykes and Garvey[1] used Slater perturbation theory to estimate the electric field strength across the diameter of the window using a dielectric bead as the perturbing object by relating the field strength to the observed frequency shift. It is hoped to extend this technique to cover the whole of the window surface and, using differently shaped perturbing objects in varying orientations, to gain some information about the field direction (see section 4.2). It may also be possible to use a conducting bead or wire loop to couple the magnetic field. Dykes and Garvey used their electric field strength estimates to arrive at a figure for the heat input to the window. More accurate mapping of the field pattern over the window aperture could

refine this estimate but more significantly it could be used to produce a thermal model of the heat flow in the window and thus produce a reasonable estimate of the temperature distribution which could in turn be used to imply the stresses due to differential expansion (see section 4.5).

3.3 Liquid Crystal and Thermal Imaging

An alternative method of looking at the field distributions in waveguides etc. is to use a thin resistive sheet, coated with a temperature-sensitive paint or stuck to a temperature-sensitive liquid crystal sheet. The sheet heats up locally according to $|E|^2$ and the visible temperature distribution yields information about the fields. It is relevant in this case of course to look at the heating directly as this is a major contribution to window failure. Laying a sheet of resistive-backed liquid crystal in the plane of the window or even sticking it to the window surface could diractly show the localised temperature distribution over the window. Pure resistive sheet would setimate ohmic loss but sticking the liquid crystal straight onto the window would also show dielectric loss. If the method is sensitive enough it may be possible to see the difference between a clean window and one contaminated by conducting films through use in the SRS.

A more flexible way to look at window heating would be the use of an infra-red camera mounted to view the top of the window, through a small hole in the waveguide opposite, or the vacuum side from the port opposite the window (usually containing the tuning plunger) if a suitably infra-red transparent window can be found. A compromise might be the use of infra-red film in a conventional camera. Thermal imaging would have the advantage that it is directly viewing the temperature of the window material and that there is no likelihood of the method perturbing the system, which is possible with resistive or dielectric sheets.

3.4 Analytical Solutions

For simple waveguide discontinuities it is often possible to derive a complete analytical solution of the fields within them by matching the wavefunction boundary conditions at all points or by matching up higher order modes, but with large apertures and realistic thicknesses of the aperture as

in the SRS case, the situation becomes too complicated for a neat analytical or mode series solution. The process of modal analysis requires careful applications although with computer assistance it may be possible to find a finite or converging series of higher order modes. The methods for such modal analysis and the criteria for converging on a real solution have been the subject of much investigation. The volume and depth of literature is rather too great to give a full account here; however, it is possible to outline some of the techniques available. Wexler[35] describes a method for solving waveguide discontinuities by summing normal propagation modes, allowing the modelling of thick irises in waveguide. Masterman et al[36] describe the problems of solving an infinitely thin iris, which may have some relevance because they illustrate how to terminate an infinite series of higher order modes and still obtain meaningful results.

Harrington and Mautz[37] describe a method for approaching the coupling betweens two arbitrary regions by an aperture, by formulation of "generalised aperture admittance operators", one for each region.

Lee et al[38] apply themselves to the criteria for convergence of a computer modal analysis and suggest some guidelines.

Another approach is to attempt to describe the problem using a network analogy, e.g. as used by Hu[39] to determine the characteristics of an arbitrary waveguide system with multi-port side couplings.

All these approaches are necessarily highy complex and require careful study of their methods, accuracy, limitations and fundamental assumptions before a choice can be made as to which is/are best applied to the SRS waveguide cavity aperture problem.

Hughes[6] attempted to relate visible marking of the window with the field distribution and noted that the magnitude of the electric field squared (i.e. proportional to dielectric loss and heating) bears some resemblance to the shape of the "tiger skin" mark. However, he assumes the window aperture to be a short length of cut-off waveguide, except within the window itself where it is above cut-off in the TE_{11} mode. Clearly, the situation is more complex than this but it is worth trying to relate any model to the observa-

ble effects on the window such as the tiger skin mark, white spot etc.

3.5 Numerical Solutions (and electron trajectory prediction)

Apart from using computers to solve modal analysis simulations, it is possible to use computer numerical methods to approach the problem of field mapping from a different direction. If sufficient information is known about the electric and magnetic fields (and charge distribution if applicable) at the boundary of a region (e.g. a simple resonant cavity) it is possible to apply a mesh-analysis technique to solve for the field at any high point within the cavity. This is the basis for many cavity design programs[40] where the r.f. characteristics of a cavity (resonant frequency, R/Q etc.) can be found on a computer without resorting to cold test work.

The limitation of this method is the resolution of the mesh that can be handled by the computer. Large numbers of mesh points generally yield better results but at the expense of running time, especially if a three dimensional mesh is needed.

It may be possible to perform a mesh analysis in the region of the window aperture between the fairly well established fields in the cavity and the waveguide. Such an analysis is more likely to converge on the right answer if a good estimate of the field is used as the starting values in the mesh, and it will also save on running time.

Once a field solution is obtained, whether by mesh analysis or analytically, the computer can be employed again in the prediction of secondary electron phenomena. It is relatively straightforward (though potentially demanding of computer time) to use a predictor-corrector type of method to track electrons through fields even when they are varying with time and displacement as in a real cavity situation. Ben-Zvi et al[41] used electron trajectory predictions, along with a "Monte-Carlo" method to simulate backscattering and secondary emission from surfaces, to predict the multiplication of electrons in a superconducting cavity. Their primary aim was to study the production of x-rays in such collisions and their results tied in extremely well with experimental observations in the form of x-ray photographs. An unexpected result of the computer simulation was the prediction of the accumulation of low energy electrons around the cavity walls (fig.4) which was found to be the case upon experimental investigation, further supporting the validity of the prediction. It was previously thought by Hughes that when tracking electrons emitted from the window, those lost to the bulk of the cavity could be ignored. Clearly this may not be the case if the surface condition of the cavity is capable of supporting secondary emission, and a suitable phase/voltage condition exists.

It is hoped that using the most complete field description possible, electron tracking will show some sort of multipactor on or around the window, to tie in with observed effects, or at least some sort of secondary electron avalanche migration which could explain surface charging.

Lyneis et al[42] successfully used an electron trajectory prediction program to simulate multipactor in a superconducting cavity and, using the program, redesigned the shape of the cavity (sharpening the corners) to minimise it. Tests on such a cavity revealed that multipactor was in fact eliminated.

4. DIRECTION OF INVESTIGATION

4.1 General

The investigation will have to approach the problem in a variety of ways. In the short term these involve:

1. Establishing the field patterns around the aperture by r.f. measurements, including perturbation techniques and liquid crystal/thermal imaging, and through analytical and numerical solutions such as mode matching and mesh analysis.
2. Developing multipactor modelling techniques by electron trajectory tracking methods.
3. Relating theoretical and experimentally observed loss mechanisms to window temperature distribution and thermal stress models.
4. Evaluating the pro's and con's of various antimultipactor coatings and measures and tying all phenomena in with high power tests in the spare cavity.

4.2 R.f. Field Mapping

It is intended to extend the perturbation technique of Dykes and Garvey to map over the whole window surface by modifying the waveguide section over the window to accept a sliding bar-in-a-slot arrangement (taking care not to disturb the waveguide currents) (see fig.5) so that the dielectric bead can be pulled across chords parallel to the diameter, along the axis of the beam. It may be possible to use a similar perturbation method below the window if a mechanical support can be contrived. Also using rods of dielectric for the perturbing object in different orientations may yield information about the direction of the field.

4.3 Analytical Field Mapping and Numerical Analysis

It would be desirable to derive some sort of analytical or hybrid analytical/numerical solution for the fields in the aperture region to check with experimental results and model heating and electron phenomena as already described. It is intended to pursue investigations into mode matching techniques etc. with a view to formulating a model of the SRS waveguide cavity system. If such a solution is possible it would be a great aid to understanding the r.f. behaviour and modelling the electron trajectories within the vacuum because the fields can be found anywhere, not just at the nearest mesh point. It is also hoped to attempt a mesh analysis for the window area either based on the r.f. measurement data or from the "known" boundary conditions somewhere in the waveguide and cavity. This may yield detailed information about the fields close to the window area, particularly useful if a good analytical solution is not possible.

4.4 Electron Tracking and Multipactor Modelling

Having hopefully gained fairly detailed information about the electric and magnetic fields throughout the vacuum region around the window aperture it should be possible to track electrons around the window area and look for regions where charge concentration, multipactor or high energy bombardment seem to occur (other experimenters have had good success with this, see section 2.4). A check may be applied to any predictions by looking for x-rays which can be predicted by the model, both in strength and distribution around

the cavity, and heating effects. If a model can be shown to be closely representative of the observed multipacting in the SRS cavities, or indeed within a klystron output window assembly, this will go a long way towards the ultimate solution of the window failure problem since any anti-multipactor, anti-charging or other loss reduction measures could be evaluated theoretically before being put to the test. This rather tall order will undoubtedly require a suite of programs which may turn out to be both complicated and expensive of computer time but if respectable results are the end product the method will be more than justified.

4.5 Thermal Analysis and Stress

Assuming the successful description of all the major contributing loss mechanisms it should be possible to establish a heat input profile for the window volume and by a numerical heat flow model, taking into account the temperature variation of such parameters as thermal conductivity, converge on an equilibrium temperature profile. Furthermore from this information (which can be compared with thermal imaging data) it should be possible to diagnose thermal stresses within the window material and even predict the failure mechanism, taking into account temperature variation of mechanical features such as UTS and thermal expansion coefficient. This could be checked by doing a destructive test of a used window on the test cavity.

5. CONCLUSION

This preliminary review of the problem has confirmed that the window failure is a complicated combination of mechanisms and suggests several areas for further investigation. The research will probably pursue parallel paths of experimental work (on the test cavity and window coatings), theoretical pursuit of an analytical solution of waveguide and cavity window fields, and the development of a computer model of cavity and window behaviour including electron trajectory plotting and other losses.

Due to the time delays in arranging the use of equipment and setting up times, an experimental program of some sort will have to be drawn up as soon as possible.

REFERENCES

1. D.M. Dykes and T. Garvey, "Cavity window field measurements", SRS/APN/84/59.
2. D.H. Priest and R.C. Talcott, "On the heating of output windows of microwave tubes by electron bombardment", IRE Trans. Electron Devices, July (1961) 243.
3. V.D. Shemelin, "Effect of the intrinsic magnetic field of a volume resonator on the secondary electron discharge in it", J. Appl. Mech. Tech. Phys. (USA), (22)5, (1981) 606.
4. W.H. Kohl, "Handbook of materials and techniques for vacuum devices". (Reinhold, New York: 1967)
5. Microwave Engineers Handbook, Vol.II.
6. E.A. Hughes, "Possible causes of some visible cavity input window phenomena", SRS/APN/84/56.
7. D.M. Dykes, T. Garvey, D.E. Poole and B. Taylor, "SRS r.f. windows", Daresbury Laboratory Preprint, DL/SCI/P463A.
8. A. Kelier and F. Körösy, "The volatile fatty acid salts of monovalent copper and silver", Magy. Tech. II(12), (1948) 127.
9. A.J. Hatch and B.F. Williams, "The secondary electron resonance mechanism of low pressure high frequency gas breakdown", J. Appl. Phys. 25, (4), (1954) 417; "Multipacting modes of high frequency gaseous breakdown", Phys. Rev. 112, (3), (1958) 681.
10. E.W.B. Gill and A. von Engel, "Starting potentials of high frequency gas discharge at low pressure", Proc. Roy. Soc. A, 197, (1947) 107; "Starting potentials of electrodeless discharge", Proc. Roy. Soc. A, 192, (1948) 446.
11. Hughes Aircraft Corp. (for NASA), "The study of multipactor breakdown in space electronic systems", Final report (1965), Contract NAS 5-3916.
12. M.P. Forrer and C. Milazzo, "Duplexing and switching with multipactor discharges", Proc. IRE, 50, (1962) 442.
13. E.F. Vance, "One-sided multipactor discharge modes", J. Appl. Phys. 34, (11), (1963) 3237.
14. B. Lax, W.P. Allis and S.C. Brown, "The effects of magnetic field on the breakdown of gases at microwave frequencies", J. Appl. Phys. 21, (1950) 1297.

15. R.J.B. Hadden, "Linear electron accelerator with a dielectric loaded waveguide", AERE GR/R 1161 (1953);
L.B. Mullet, R.E. Clay and R.J.B. Hadden, "Multipactor effect in linear accelerators and other evacuated r.f. systems, and a new cold cathode valve", AERE GR/R, 1076 (1957).
16. H.A. Schwettman, "Practical considerations in the design and operation of superconducting structures", IEEE Trans. Nucl. Sci. NS-22, (1975) 1118;
M. Broussoukaya, Nygen Tuong Viet and L. Wartski, "Etude de la décharge resonante dans des cavités réentrantes supraconductrices" (in French), Nucl. Instrum. Meth. 203 (1982) 13.
17. H. Derfler, H. Brinkschulte, F. Leuterer, J. Perchermeier and H. Spitzer, "The suppresaion of multipactors in lower hybrid antennae", Proc. 4th Int. Symp. Heating in Toroidal Plasmas, Vol.2, (1984) 1261, Published by Monotypia Franchati, citta di castello (Perugia), Italy;
E. Franconi, "Multipacting and secondary electron emission from the FT r.f. waveguide system", Ibid., pp.1201;
J. Rodney and M. Vaughan, "Multipactor in the Brambrilla Grill", Proc. IEEE, 70, (2), (1982) 203.
18. W.J. Gallagher, "The multipactor effect", IEEE Trans. Nucl. Sci. NS-26, (3), (1979) 4280;
"Further notes on the multipactor effect", IEEE Trans. Nucl. Sci. NS-32, (5), (1985) 2900.
19. W.J. Gallagher, "The multipactor electron gun", Proc. IEEE, Jan.1968 pp94-5.
20. M.P. Forrer and C. Milazzo, "Duplexing and switching with multipactor discharges", Proc. IRE, 50, (1962) 442.
21. Hughes Aircraft Corp. (for NASA), "The study of multipactor breakdown in space electronic systems", Final Report (1965) NAS 5-3916.
22. K. Bol-Sperry Gyroscope Co. (sponsored by US Navy), "The multipactor effect in klystrons", IRE Nat. Conv. (1954) record 2 pt.3, p.151.
23. L.V. Grishin and G.S. Luk'yanchikov, "Multipactor discharge with an electron velocity distribution", Sov. Phys. Tech. Phys. 21, (3), (1976) 307.
24. R.A. Shatas, J.F. Marshall and M.A. Pomerantz, "Dependence of secondary electron emission upon angle of inoidence of 1.3 MeV primaries", Phys. Rev. 102, (3), (1956) 682.

25. R.E. Simon and B.F. Williams, "Secondary electron emission", IEEE Trans. Nucl. Sci. NS-15, (1968) 167.

26. K. Kanaya and K. Kawakatsu, "Secondary electron emission due to primary and backscattered electrons", J. Phys. D: Appl. Phys. 5, (1972) 1727.

27. P.H. Dawson, "Secondary emission yields of some ceramics", Communications, April (1966) 3644.

28. H. Padamsee and A. Joshi, "Secondary electron emission measurements on materials used for superconducting microwave cavities", J. Appl. Phys. 50, (2), (1979) 1112.

29. R.C. Talcott, "The effects of titanium films on secondary electron emission phenomena in resonant cavities and at dielectric surfaces", IRE Trans. Electron Devices, 19, (5), (1962) 405.

30. R. Hayes, "Research on microwave window multipactor and its inhibition", NTIS Database (AD-456 965 NTIS 66002006) 30 June (1964).

31. D. Ruzic, R. Moore, D. Manos and S. Cohen, "Secondary electron yields of carbon coated and polished stainless steel", J. Vac. Sci. Technol. 20, (4) (1982) 1313.

32. E. Franconi, "Secondary electron yield of graphite and TiC coating", Fus. Technol. (USA), 6, (1984) 414.

33. J. Timberlake, S.A. Cohen, C. Crider, G. Estepp, W. Hooke, D. Manos, J.Stephens and M. Ulrickson, "Surface modifications of PLT lower hybrid waveguides to improve operations", J. Vac. Sci. Technol. 20, (4), (1982) 1309.

34. J. Halbritter, "On conditioning: Reduction of secondary and r.f. field emission by electron, photon or helium impact", J. Appl. Phys. 53, (9), (1982) 6475.

35. A. Wexler, "solution of waveguide discontinuities by modal analysis", IEEE Trans. Microwave Theory Tech. 15, (9), (1967) 508.

36. P.H. Masterman, P.J.B. Clarricoats and C.D. Hannaford, "Computer method of solving waveguide-iris problems", Electron. Lett. 5, (2), (1969) 23.

37. R.F. Harrington and J.R. Mautz, "Characteristic modes for aperture problems", IEEE Trans. Microwave Theory Tech. 33, (6), (1985) 500.

38. S.W. Lee, W.R. Jones and J.J. Campbell, "Convergence of numerical solutions of iris type discontinuity problems", G-AP Int. Symp. Columbus, OH, USA, (1970) 384.

39. Q.L. Hu, "The transmission coefficient for an arbitrary waveguide system with multiport side couplings", Int. J. Electronics, 56, (2), (1984) 197.

40. H.C. Hoyt, "Computer designed 805 MHz proton linac cavities", Rev. Sci. Instrum. 37, (6), (1966) 755.

41. I. Ben-Zvi, J.F. Crawford and J.P. Turneaure, "Electron multiplication in cavities", IEEE Trans. Nucl. Sci. NS-20, (1973) 54.

42. C.M. Lyneis, H.A. Schwettman and J.P. Turneaure, "Elimination of electron multipacting in superconducting structures for electron accelerators", Appl. Phys. Lett. 31, (8), (1977) 541.

Table 1. Mechanical and thermal properties of alumina and beryllia (metric values converted from data from refs.(4) and (5)).

Temperature (except where shown otherwise) (°C)	Thermal conductivity (J/cm s °C)	Thermal expansion (cm/cm °C × 10^{-7})	Specific heat capacity (J/g °C)	Ultimate tensile strength (N/mm^2)	Modulus of elasticity $N/mm^2 \times 10^3$
Alumina					
23	0.352	73	0.80	293	37
500	0.096	75	1.27(1050)	146(600)	35(600)
1000	0.059	85	1.26(1200)	84	32
1500	0.059	95	1.34(1400)	59(1200)	27(1200)
Beryllia					
23	2.18	80	1.0	118	30
500	0.63	80	1.9	44(800)	29(600)
1000	0.21	90	2.2(900)	24	22
1500	0.15	100	-	20(1200)	13(1200)

Table 2. Electrical properties of alumina and beryllia

	Temperature (°C)	Dielectric constant	Loss tangent[a] (tan δ)	Resistivity (Ω)	Ref.
Al_2O_3	25	9.6	0.0001	> 10^{14}	
AD995	500	10.4	0.0002	1.4 × 10^9	4
(1 GHz)	800	11	0.0003	4 × 10^7	
(Av 1-30 GHz)	25	~9	0.0006 - 0.0007		5
BeO	25	6.7	-	10^{16}	
(1 MHz)	500	-	-	10^9	4
	800	-	-	10^7	
(Av 1-30 GHz)	25	~4	~0.0005	-	5

	D.C. Breakdown field (V/mm)	Sample size (mm)	Maximum operating temperature (°C)
Alumina (average)	230	250	1400-1900
AD94 (94% pure)	600	10	1700
Beryllia (average)	240-250	250	1700-1850
BD995 (99.5% pure)	700	10	1850

[a] $\left[\tan\delta = \frac{\text{real part of } \epsilon}{\text{imag. part of } \epsilon}, \text{ power loss/unit vol.} = \epsilon_o \epsilon_r \omega E^2 \tan\delta\right]$

Table 3. Some values of the SEC[(a)] for alumina and beryllia

Al_2O_3	1.5 - 9	primary voltage for max. secondary emission	350 - 1300 V
BeO	~ 3.4	primary voltage for max. secondary emission	~ 2 kV

[(a)] SEC increases with angle of incidence θ as sec θ.

FIGURE CAPTIONS

Fig.1 SRS window mounting arrangement.

Fig.2 Standing wave patterns in waveguide.

Fig.3 Typical klystron window arrangement.

Fig.4 A typical computer plot of the trajectories in z-r space of ten initial electrons and their second and higher generation electrons produced by the electron multiplication simulation program.

Fig.5 Modifications to waveguide/cavity transition for perturbation measurements.

Lower position, coupling factor = 6

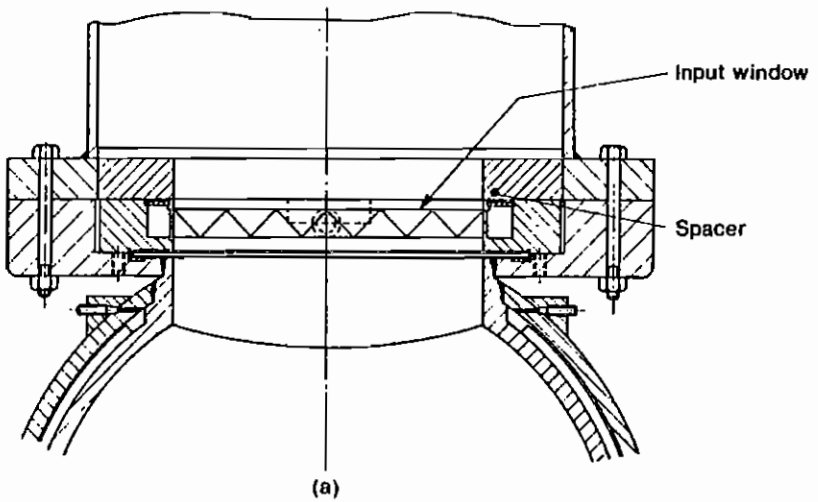

(a)

Raised position, coupling factor = 3

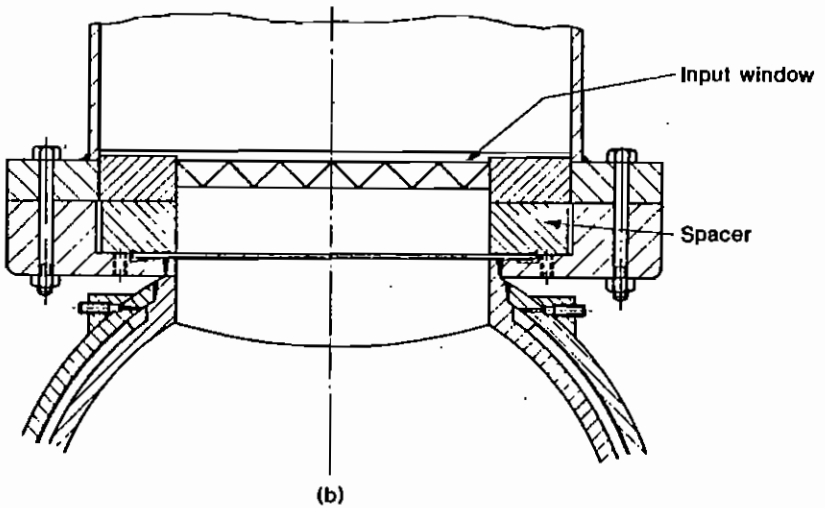

(b)

Fig. 1

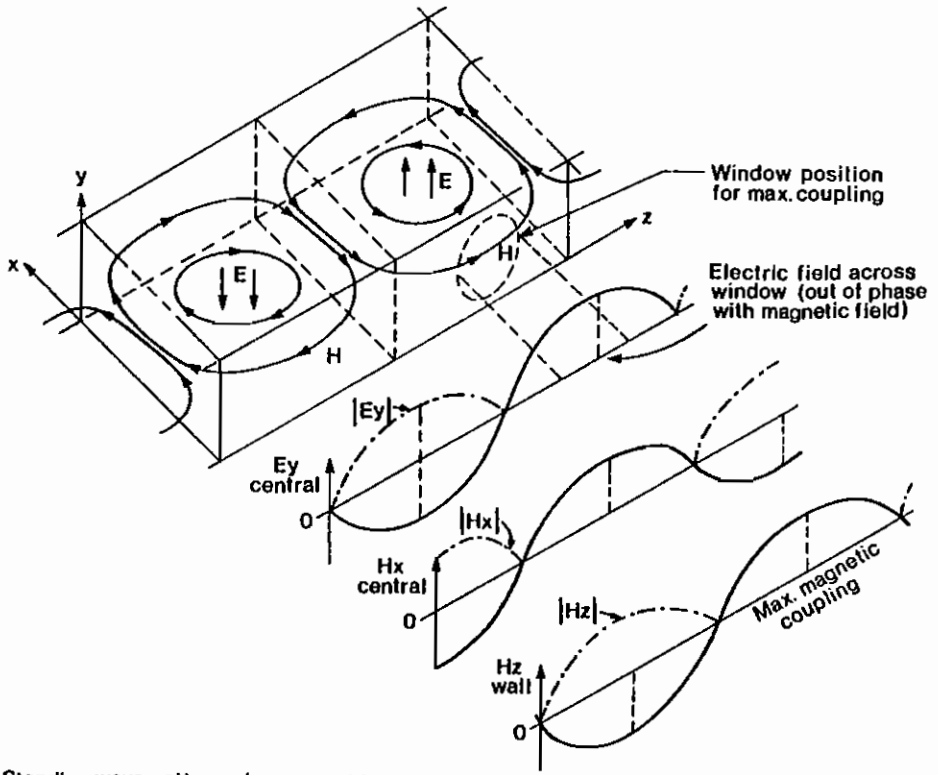

Standing wave patterns in waveguide (H_{10} mode)

Fig. 2

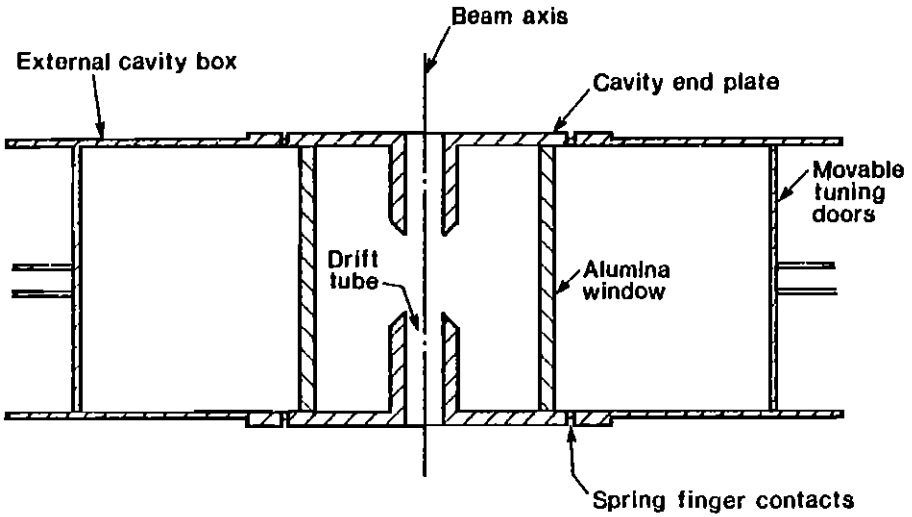
Beam axis
External cavity box
Cavity end plate
Movable tuning doors
Drift tube
Alumina window
Spring finger contacts

Fig. 3

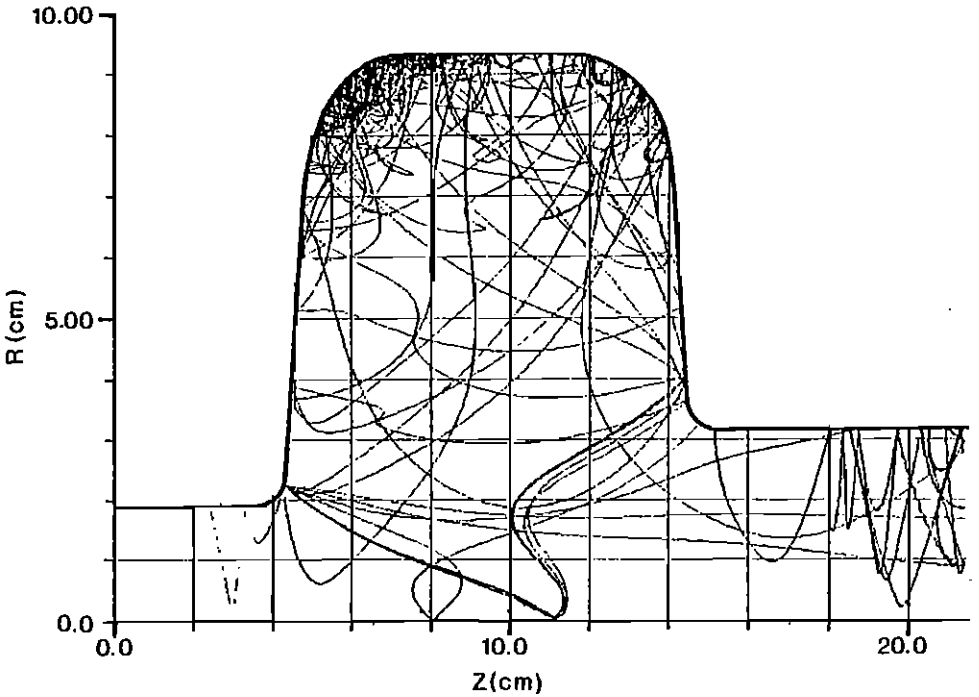
10.00
5.00
0.0
R (cm)
0.0
10.0
20.0
Z(cm)

Fig. 4

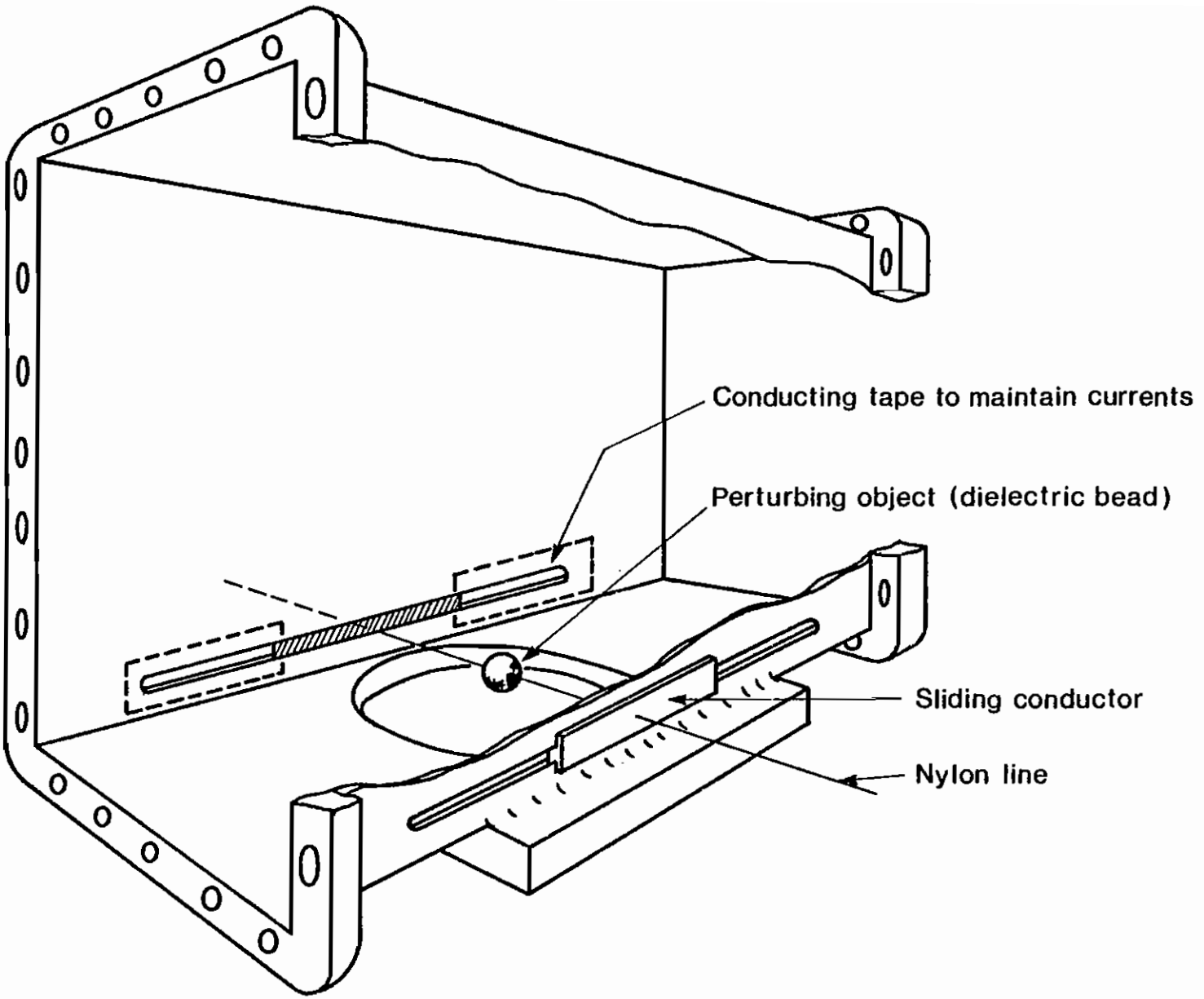
Conducting tape to maintain currents
Perturbing object (dielectric bead)
Sliding conductor
Nylon line

Fig. 5